Archives of Biochemistry and Biophysics 587 (2015) 38–47

Contents lists available at ScienceDirect

Archives of Biochemistry and Biophysics

journal homepage: www.elsevier.com/locate/yabbi

Homophilic interaction and deformation of E-cadherin and cadherin 7 probed by single molecule force spectroscopy

Fei Wu [a, b, c, 1], Prashant Kumar [d, 1], Chen Lu [c], Ahmed El Marjou [f], Wu Qiu [a, b], Chwee Teck Lim [c, g], Jean Paul Thiery [d, e], Ruchuan Liu [a, b, c, *]

[a] College of Physics, Chongqing University, No.55 Daxuecheng South Rd., Shapingba, Chongqing 401331, China
[b] Department of Physics, National University of Singapore, 2 Science Drive 3, Singapore 117542, Singapore
[c] Mechanobiology Institute, National University of Singapore, 5A Engineering Drive 1, Singapore 117411, Singapore
[d] Institute of Molecular and Cell Biology, Proteos, Singapore 138673, Singapore
[e] Department of Biochemistry, Yong Loo Lin School of Medicine, National University of Singapore, 8 Medical Drive, Singapore 117597, Singapore
[f] Institut Curie CNRS144, Paris 75005, France
[g] Department of Bioengineering, National University of Singapore, 9 Engineering Drive 1, Singapore 117576, Singapore

ARTICLE INFO

Article history:
Received 23 June 2015
Received in revised form
8 October 2015
Accepted 9 October 2015
Available online 24 October 2015

Keywords:
Force spectroscopy
Cell adhesion
Atomic force microscopy
Magnetic tweezers

ABSTRACT

Cadherin-mediated adhesion plays a crucial role in multicellular organisms. Dysfunction within this adhesion system has major consequences in many pathologies, including cancer invasion and metastasis. However, mechanisms controlling cadherin recognition and adhesive strengthening are only partially understood. Here, we investigated the homophilic interactions and mechanical stability of the extracellular (EC) domains of E-cadherin and cadherin 7 using atomic force microscopy and magnetic tweezers. Besides exhibiting stronger interactions, E-cadherin also showed more efficient force-induced self-strengthening of interactions than cadherin 7. In addition, the distributions of the unbinding forces for both cadherins partially overlap with those of the unfolding forces, indicating that partial unfolding/deformation of the cadherin EC domains may take place during their homophilic interactions. These conformational changes may be involved in cadherins physiology function and contribute to the significant differences in adhesive strength mediated by type I and type II cadherins.

1. Introduction

Selective and robust cell–cell adhesion plays a key role in maintaining tissue structural integrity and specific architecture in multicellular organisms [1,2]. In most tissues, cell–cell adhesion is dominated by a class of transmembrane proteins named cadherins [1,2]. Dysregulation of cadherin function correlates with tumour cell invasion and distant dissemination [1–4]. The cadherin superfamily comprises distinct families and subfamilies [5,6]; one of these is the classical cadherins. E-cadherin, the prototypic member of classical type I cadherins, is an essential component of epithelial adherens junctions and contributes to a fully polarized state in the cell through the formation of a circumferential actin belt. In contrast, classical type II cadherins, such as cadherin 7, show significantly weaker adhesion and are mainly expressed in mesenchymal tissues [6,7].

Type I and type II cadherins demonstrate similar domain organization: a cytoplasmic region, a transmembrane region, and an extracellular region [8,9]. The primary sequence of the extracellular region differs significantly between type I and type II cadherins [10]. The forces required to separate cell doublets expressing type II cadherins are much weaker than for those of type I-expressing cells, a property linked to their extracellular region [6]. Nonetheless, the extracellular segments of type I and type II cadherins share a similar 3D structure that comprises five tandem repeats, called extracellular cadherin (EC) domains, herein referred to as EC1 to EC5. Each EC domain consists of about 110 amino acids forming seven β-strands that are organized into two β-sheets [5,11,12].

Crystallographic data suggest the formation of X-dimers and strand-swapping dimers by the homophilic interaction of classical

Abbreviations: EC, extracellular cadherin; EC1 to EC5 domains, the first to the fifth extracellular cadherin domains; AFM, Atomic Force Microscopy; SMD, Steered Molecular Dynamics; TIRF, Total Internal Reflection Fluorescence.

* Corresponding author. College of Physics, Chongqing University, No.55 Daxuecheng South Road, Shapingba, Chongqing 401331, China.
E-mail address: phyliurc@cqu.edu.cn (R. Liu).

[1] Both authors contribute to this paper equally.

http://dx.doi.org/10.1016/j.abb.2015.10.008
0003-9861/

type I cadherins *in vitro* [12–14]. In a two-step adhesive binding experiment, cadherins were shown to initially form X-dimers and then convert to strand-swapping dimers [12]. A similar pathway were also proposed by Rakshit et al., as in the atomic force microscopy (AFM) studies [15], they found that strand-swapping dimers formed slip bonds, and X-dimer of E-cadherin formed catch bonds [15]. The latest steered molecular dynamics simulations results suggest that tensile force can deform cadherin EC domains to form long-lived hydrogen bonds to tighten the X-dimer contact [16]. Crystallographic studies also show that type II cadherins form similar strand-swap dimers [13,14]. In their strand-swapping dimers, the buried accessible surface area was found larger than that of type I cadherins [13,14] and, the dissociation constants (k_d) measured by ultracentrifugation [17] imply that the binding energy of type II cadherins is higher than that of type I cadherins. On the contrary, type I cadherins expressed cells show stronger unbinding forces [6,7]. Nevertheless, direct comparison between type I and type II cadherins at the molecular level is lacking, while this is important for understanding the distinct adhesion mechanism between them.

In the AFM study of E-cadherin X-dimers and strand-swapping dimers, Rakshit et al. proposed a model of reorientation of the EC domains by tensile forces to lock the dimer more tightly by an alternate binding site as the mechanism of the catch-bond behaviour. Meanwhile, quite a few studies also indicate that force plays important role in assisting cadherin-mediated adhesion processes. E-cadherin-mediated adhesion occurs under an actomyosin-generated tension force *in vivo* [18], force can enhance E-cadherin-mediated adhesion [19–21], and force can also increase the junction size in cadherin adhesions [22,23]. In addition, studies indicated that the cells can respond to the activation of E-cadherin EC domains (conformational change for binding) to regulate adhesion [24]. Therefore, EC domains and the homophilic interactions of their pairs response to mechanical forces is essential for cell–cell interaction.

Here, we used AFM to compare the homophilic interactions between E-cadherin and cadherin 7 at the single-molecule level varied under the external force dynamics. While both cadherins showed slightly time-dependent strengthening in their homophilic interactions, the strengthening effect by additional mechanical stretching is much more noticeable for E-cadherin than for cadherin 7. The elasticity of the EC domains of both cadherins were also carried out using AFM and magnetic tweezers, and the results indicated that the force to partially unfold/deform the EC domains showed a larger overlap with the unbinding force of the dimers for E-cadherin than cadherin 7.

2. Material and methods

2.1. Protein cloning

The Ecad and Cad7 genes were cloned into pFB-Sec-NH vector (Addgene) using ligation-independent cloning [25]. The forward and reverse primers for Cad7 were 5' –TACTTCCAATCCATGAGCTGGGTTTGGAATCAGTTC-3′ and 5′-TATCCACCTTTACTGTCACTCTGCATTGCAGGTCTGG-3′, and for Ecad, 5′-TACTTCCAATCCATGGACTGGGTCATCCCTCCC-3′ and 5′-TATCCACCTTTACTGTCACGCCTTCATGCAGTTGTTGA-3'. The construct contains baculovirus gp64 signal peptide followed by an N-terminal hexahistidine tag and TEV protease cleavage site. Bacmid production, insect cell transfection and virus production were performed as previously described [26]. The early passage of virus particles (P0) was amplified to P2 and was used to infect 2 L of log phase (3 × 106 cells/ml) insect cells for recombinant protein expression. The multiplicity of infection (MOI) was kept between 2 and 3 and the culture was incubated at 140 RPM, 27 °C for 56 h.

2.2. Protein purification

The culture was spun at 4000 × g for 30 min and the supernatant was collected. Protease inhibitor cocktail (Calbiochem) was added to the media (100 μl per 1 L media). For optimal binding, the pH of the supernatant was adjusted to 7.5 using a solution of 500 mM Tris pH 8.0 and 1.5 M NaCl. Ni-NTA Agarose (10 ml; Life Technologies) was added to the supernatant and incubated with rotation at 80 RPM for 1 h (4 °C). The supernatant was then subjected to second protein absorption with 5 ml Ni-NTA beads. The beads were collected and loaded into gravity columns and washed with 20 column volumes (CV) of wash buffer (50 mM Tris, pH 8.0, 500 mM NaCl and 2 mM imidazole, pH 8.0). The target protein was eluted with elution buffer (50 mM Tris, pH 8.0, 500 mM NaCl and 250 mM imidazole pH 8.0). Two CV fractions were collected per time until no protein was detected (absorbance, 280 nm) in the elution buffer. The eluted protein was subjected to buffer exchange (PD10 column, GE Healthcare) and digested with TEV protease (1:40 ratio of mg TEV protease:mg protein) at 4 °C overnight [27]. The sample was then loaded onto a gravity column packed with Ni-NTA agarose beads for the removal of the free His-Tag and TEV protease. The flow-through containing the target protein was collected. The fractions containing the target protein were collected and concentrated to 5 ml using 10K MWCO concentrator (Vivaspin 20 ml, Sartorius Stedim Biotech) before being subjected to size-exclusion chromatography (SEC). SEC was conducted in the AKTA Xpress system (GE Healthcare) using a HiLoad 16/60 200 Superdex prep-grade column equilibrated in GF buffer (20 mM HEPES, 300 mM NaCl, 10% (v/v) glycerol). Elution peaks were collected in 2 ml fractions and the purity of the protein was analysed on SDS-PAGE. The protein sample was again concentrated using a 10K MWCO concentrator (Vivaspin 20 ml, Sartorius Stedim Biotech).

2.3. Buffers and substrates

Unless otherwise stated, a 25 mM HEPES, 125 mM NaCl and 3 mM $CaCl_2$ buffer with a pH adjusted to 7.2 was used. Quartz (UQG optics, Cambridge, Cambridgeshire, UK) slides were cleaned by washing successively in a sonicator with deionized water, ethanol and deionized water again for 20 min each step, and then treated by air plasma (Expanded Plasma Cleaner, Harrick Plasma, St. Ithaca, NY, USA) for 5 min before use.

Three different coating methods were used in experiments. For AFM unbinding experiments, NTA/Ni^{2+}-coated AFM cantilever and quartz slides were prepared. The cantilever and slides were coated with biotin by incubating in 0.1 mg/ml biotin-labelled BSA (Sigma–Aldrich St. Louis, MO, USA) overnight. The 0.4 mM biotin-PEG-SVA (Laysan Bio, Arab, AL, USA) solution was labelled with NTA by reacting with 1 μg/mL Nα,Nα-bis(carboxymethyl)-L-lysine hydrate (Sigma Aldrich) overnight. The NTA-labelled PEG was diluted and mixed with 0.1 mg/mg streptavidin (Sigma Aldrich) at a 1:4 M ratio for 30 min. Finally, the biotin-coated cantilever and slides in the first step were coated with this mixture solution for 30 min, followed by 100 mM $NiSO_4$ for 30 min.

For AFM unfolding experiments, NTA/Ni^{2+}-coated quartz slides were prepared in five steps by incubating sequentially in 1 M NaOH solution for 15 min, propylmethyldimethoxysilane (Alfa Aesar, Ward Hill, MA, USA) solution (1% propylmethyldimethoxysilane, 4% water, 95% ethanol) for 15 min; 0.05% glutaraldehyde (Sigma Aldrich) solution for 1 h; 1 μg/mL Nα,Nα-bis(carboxymethyl)-L-lysine hydrate solution for 30 min, and finally in 100 mM $NiSO_4$ solution for 30 min [28]. The slides were washed thoroughly with deionized water between the steps.

For magnetic tweezers unfolding experiments, biotin-coated slides were prepared by incubating in 1 M NaOH solution for 15 min, propylmethyldimethoxysilane solution for 30 min, and 10 mM HEPES (pH = 7.2) buffer with a mixture of 5 mM methyl-PEG-SVA (Laysan Bio) and 5 nM biotin-PEG-SVA (Laysan Bio) [29] for 4 h.

2.4. AFM experiments

AFM unbinding experiments by Shi et al. have shown that the unbinding forces between varied length of EC domains of C-cadherins are different, suggesting that all 5 EC domains contribute to the strength of homophilic interactions of cadherins [30]. Thus, we used the full extracellular part of cadherins in this report. AFM experiments were performed using a commercial AFM (JPK Nanowizard II, JPK Instruments, Berlin, Germany) with the silicon tip cantilever (HYDRA2R-100NG, The Applied Nano Structure Inc., Santa Clara, CA, USA). In experiments, EC1-5-His_6 protein and the NTA-Ni^{2+}-coated cantilever/quartz slides were used, where the His-tag terminal of the protein molecule was expected to bind specifically with NTA-Ni^{2+} on the cantilever and slides.

In unbinding experiments, the slides were incubated with 15 μl of ~20 μg/ml protein solution in HEPES buffer for 15 min. The slides were then washed five times with buffer to remove floating protein molecules. Before an experiment, the sample was incubated for 1 h with 1 mg/ml BSA to block non-specific binding. The measurements were performed in a buffer containing 0.1 mg/ml BSA.

In unfolding experiment, the slides were incubated with 15 μl of ~20 μg/ml protein solution in buffer for 15 min and then washed five times with buffer to remove floating protein molecules.

2.5. Magnetic tweezers experiments

Solutions of 0.2 μg/mL E-cadherin biotin-EC1-5-His_6 protein and 0.2 μg/mL neutravidin (Thermo Fisher Scientific, Waltham, Massachusetts, UK) were mixed at a molar ratio of 1:1 for 30 min and then added to biotin-coated quartz slides for 30 min. A buffer containing 2% BSA was introduced for approximately 2 h to further block non-specific binding sites. Carboxyl group-functionalised green fluorescent magnetic beads (The Bangs Laboratories, Fishers, IN, USA) with a diameter of ~2.8 μm were treated with a mixture of 50 mg/ml sulfo-NHS (Alfa Aesar) and 50 mg/ml EDC (Thermo Fisher Scientific) in 50 mM MES (pH 4.7, Sigma Aldrich) activation buffer for 20 min prior to incubation with 1 μg/ml Nα,Nα-bis(carboxymethyl)-L-lysine hydrate for 4 h. The NTA-coated beads were then incubated with a solution of 100 mM $NiSO_4$ for 1 h and stored in a HEPES buffer containing 2% BSA. Before experiments, NTA-Ni^{2+}-coated beads were incubated on quartz slides with biotin-EC1-5-His_6 proteins for 1 h, and the His-tag at the C-terminus of the protein was expected to bind to NTA-Ni^{2+} via the beads. Any residual unbound protein was washed away with a HEPES buffer containing Ca^{2+} ions prior to measurements.

Magnetic tweezers experiments were performed on a home-built magnetic tweezers/evanescent nanometry [31]. The combination of a permanent magnet, I×71 Total Internal Reflection Fluorescence (TIRF) microscope (Olympus, Tokyo, Japan) and QuantEM 512sc camera (Photometrics, Tucson, AZ, USA) was controlled by codes written in Igor Pro (Wavematrics, Lake Oswego, OR, USA). The force calibration was based on equi-partition theorem [32]. A constant unfolding force around 5 ± 3 pN (SD) was applied to the beads by the magnetic tweezers and protein extension was monitored using the TIRF microscope [31].

2.6. Excluding the interference of linkage breaking

In our AFM unbinding experiments, linkages, including NTA-His_6 binding, SVA-NH2 binding, biotin-streptavidin binding and BSA adsorption were utilised. These linkages have been widely utilised in previous AFM single-molecule experiments. Among them, NTA-His6 linkage shows rupture forces around 200 pN under similar loading rates as in our experiments [33]. Additionally, in our unfolding experiments where cadherins molecules were immobilized on the slides via NTA-His6 linkage, the average detaching force was 195 pN. These forces are much higher than the unbinding force (<120 pN) measured in our experiments. SVA-NH2 and biotin-streptavidin binding have been utilised in previous AFM studies on E-cadherin unbinding [15,34], whereas the absorption of BSA has been utilised to measure the unbinding force of the biotin-streptavidin linkage [35]. Thus, these linkages should be much stronger than the cadherin homophilic interactions. Therefore, the unbinding events measured in our experiments are not the rupture of the linkages that are used to immobilise cadherins on the AFM cantilever and substrates.

In AFM unfolding experiments, the linkages of NTA-His_6 binding is small and simple, so its breakage cannot contribute to the saw-tooth pattern of unfolding proteins, but cause the detachment peak in the AFM force-extension trajectories.

3. Results

AFM was used to measure the unbinding forces of homophilic interaction pairs between E-cadherin and cadherin 7 EC domains. The molecular elasticity of these EC domains was also investigated using AFM and magnetic tweezers; in the latter case, the stretching forces can be as low as a few pN, which is close to the *in vivo* forces borne by adhesion molecules.

3.1. Rupture force of individual homophilic pairs

In AFM unbinding experiments, EC1-5-His_6 molecules of E-cadherin/cadherin 7 were immobilized on cantilever and slides and formed bonded pairs by homophilic interaction (Fig. 1a). The average distance between neighbouring EC molecules was ~90 nm, as measured by fluorescently labelled EC molecules using the same method as described previously [34]. This is much larger than the radius of the AFM tips (~10 nm); thus, most unbinding events observed should come from individual bonded pairs. Consistently, the binding probability in our experiments was ~10%, which, according to Poisson statistics, correspond to ~95% probability of individual homophilic pairs. As a control, the deletion of EC molecules on the cantilever and the removal of Ca^{2+} ions significantly decreased the binding probability (Table S1 in File S1).

Three types of force cycles were utilised in the AFM rupture experiments: contact of 2 s and 10 s at ~10 pN (pushing) before pulling, as well as the pull-release-pull cycle (Figs. 1c and d). Typical force trajectories are shown in Figs. 1c and d, respectively. The different baseline of pushing (blue) and retracting (green) segment is caused by the shifting of AFM system and is around 10 pN. The rupture forces of E-cadherin interactions (~52 pN) were similar to those found in previous studies [34,36,37], with consideration of the different loading rates or slight variations in force calibration conditions in AFM. The histograms of the rupture forces of E-cadherin and cadherin 7 are shown in Figs. 2a–f. In all three types of force cycles, E-cadherin showed higher average unbinding force than cadherin 7 (Fig. 2g), consistent with *in vivo* measurements [6,7]. In all situations (Figs. 2a–f), there was a broad distribution of rupture forces for both cadherins, and a significant difference between Cad7 and Ecad as evident from the figures ($p < 0.0001$, by an

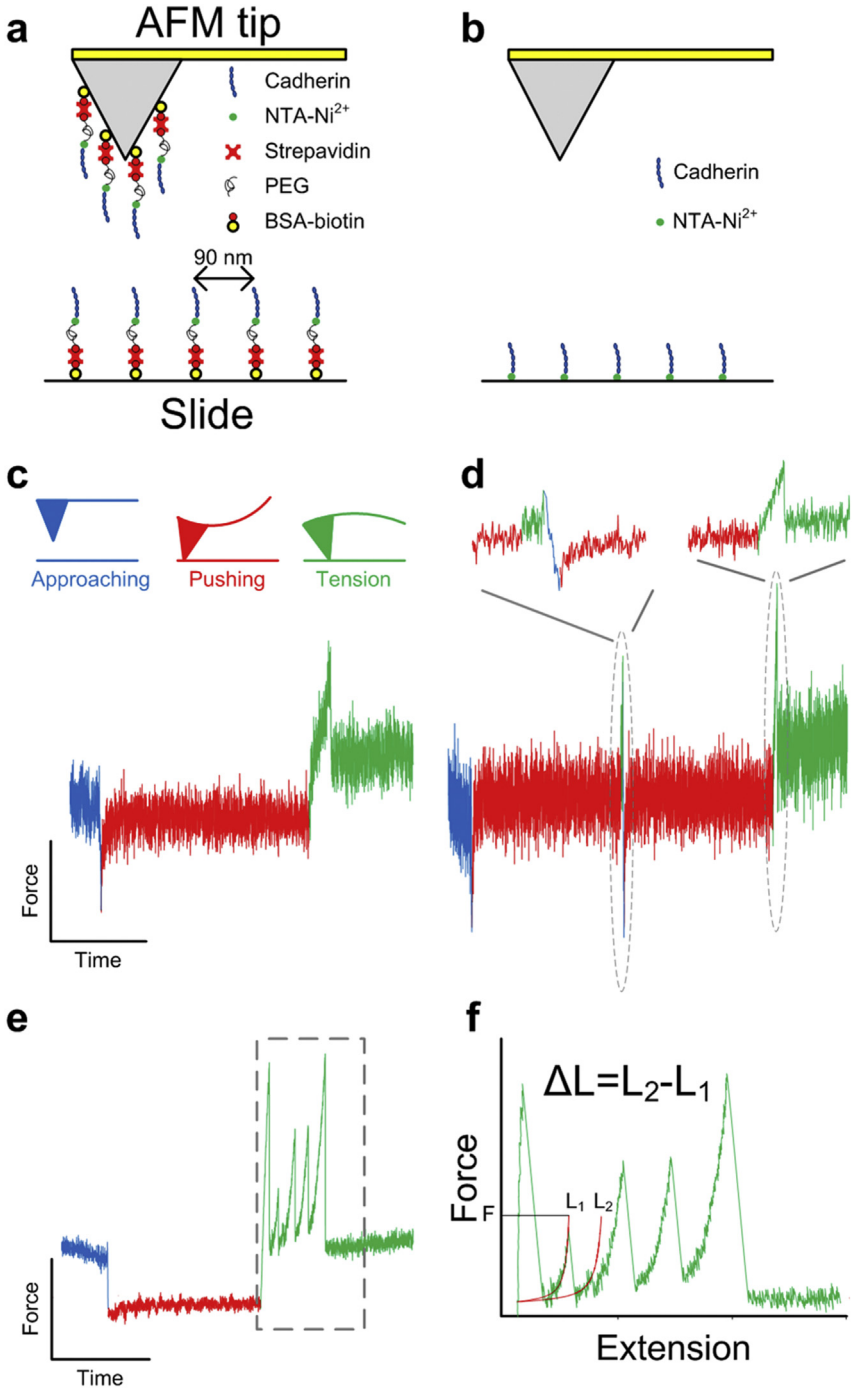

Fig. 1. Schemes of AFM force spectroscopy measurements. (a) Schematic of AFM unbinding measurements. The tip and the substrate were functionalised with PEG linker, which was linked to NTA. His-tagged protein was immobilised via Ni^{2+}-NTA at a surface density of ~120 monomers per μm^2. (b) Schematic of AFM unfolding measurements. The substrate was functionalised with Ni^{2+}-NTA, which could immobilise His-tagged proteins. (c) Typical force scan curves in short-term and long-term contact force cycles. AFM tip was pushed towards the slides to 50 pN (blue trace), and then immediately retracted to maintain 10 pN pushing force for 2 or 10 s to allow cadherins on the tip and slides to form homophilic interaction pair (red trace). Then, the tip was retracted at 600 nm/s for 1 s to detect the bond rupture force (green trace). (d) Typical force scan curves in pull-release interaction force cycles. The AFM tip was pushed towards the slides to 50 pN (blue trace), and then immediately retracted to maintain 10 pN pushing force for 2 s to allow cadherins on the tip and slides to form homophilic interaction pairs (red trace). Then, the tip was retracted until the tension force reached 25 pN (green trace) and pushed toward the slides again (blue trace), and held at 10 pN for 2 s (red trace). Finally, the tip was retracted at 600 nm/s for 1 s to detect bond rupture (green trace). (e) Typical force scan curves in unfolding measurements. In the left curve, the AFM tip was pushed towards the slides to 50 pN and held at this force for 1 s, then retracted at 600 nm/s for 1 s. Occasionally, a single molecule of protein was mechanically stretched between the tip and substrate and an unfolding curve can be observed. (f) Fitting method for force vs. extension unfolding curves. Force of the first unfolding peak was recorded as unfolding force, F. Worm-like-chain (WLC) model (red curve) was used to fit the force peaks for the contour length change ΔL [59]. (For interpretation of the references to colour in this figure legend, the reader is referred to the web version of this article.)

unpaired t-test). In all the distributions, there is a major peak at the low force region (between 20 and 40 pN), with a long tail extending into the high force region. Therefore, by considering the shape of all these distribution, we assume a boundary of 70 pN to separate the high force tail from the main distribution for comparison. The population of the high rupture force tail (>70 pN) is shown in

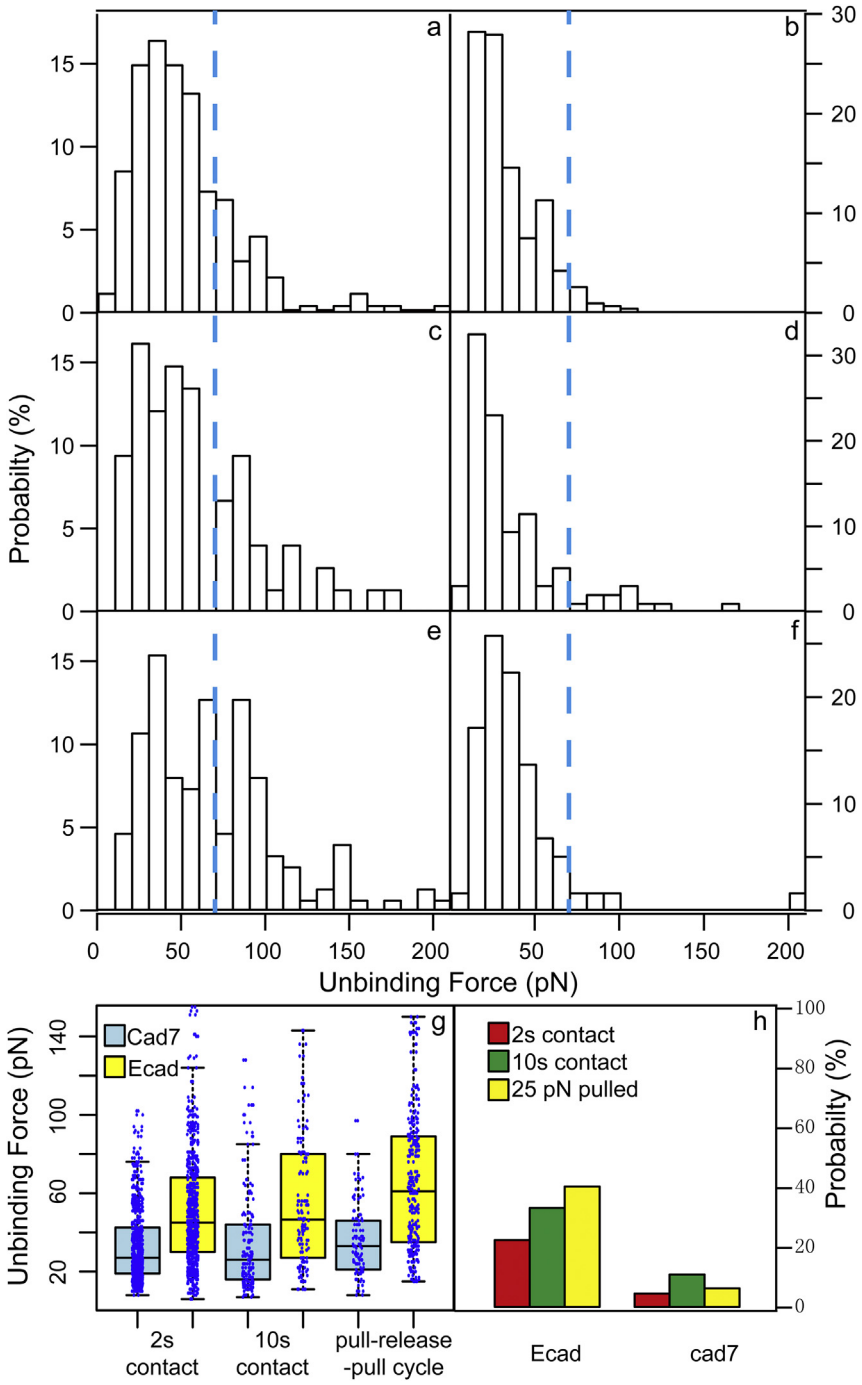

Fig. 2. Unbinding forces of curves with single force peak. (a) Unbinding force histogram of E-cadherin bonds after a 2-seconds contact. The total number of events is 407. (b) Unbinding force histogram of cadherin 7 bond after a 2-seconds contact. The total number of events is 366. (c) Unbinding force histogram of E-cadherin bond after a 10-seconds contact. The total number of events is 74. (d) Unbinding force histogram of cadherin 7 bond after a 10-seconds contact. The total number of events is 95. (e) Unbinding force histogram of E-cadherin bond in pull-release force cycle. The total number of events is 149. (f) Unbinding force histogram of cadherin7 bond pull-release force cycle. The total number of events is 58. A significant difference ($p < 0.0001$) between Cad7 and Ecad as evident from these figures, calculated by an unpaired t-test. The dash lines at a 70 pN in (a)–(f) are chosen to separate the high force unbinding events from the main force peak in the distributions. (g) The box dot plots of the unbinding force data. The bottom and top of the boxes are the first and third quartiles, the band inside the box is the second quartile (median), and the ends of the whiskers show 1.5 interquartile range (IQR) from the lower and upper quartiles, respectively. (h) Probabilities of high unbinding forces from (a)–(f). A long contact time raise the probability for both E-cadherin and cadherin 7. However, E-cadherin bonds show a more evident larger probability of high rupture forces, whereas in case of cadherin 7 bonds the probability remain a similar level.

Fig. 2h. Compared with the results obtained for the 2-sec contact, the larger probability of high rupture forces for the 10-sec contact indicated slightly strengthening of the homophilic interactions for both E-cadherin and cadherin 7. The difference between E-cadherin and cadherin 7 was distinct in the case of the pull-release-pull force cycle. For E-cadherin, the strengthening of the homophilic interaction by pre-pulling at a force of 25 pN is more evident, whereas no or only a limited effect was observed after pre-pulling for cadherin 7. To exclude the multiple binding, only force-extension curves with single force peak were taken for plotting here. The

histograms for all force-extension curves are shown in Fig. S1. We also performed control experiments on unbinding of cadherins in absence of Ca^{2+}, and observed the significantly decrement of binding probability as listed in Supporting Information table S1.

3.2. Partial unfolding of EC domains by external forces

To examine the mechanical stability of the EC domains of both cadherins, forced unfolding measurements were also carried out at the single-molecule level. The histograms of the force for the first unfolding event in each AFM trajectory are shown in Figs. 3a and b (red bars) for E-cadherin and cadherin 7, respectively. The average unfolding force of E-cadherin was only slightly higher than that of cadherin 7. The unfolding forces of the E-cadherin EC domains were similar to that of C-cadherin, also measured by AFM [38]. On the other hand, because each of the five E-cadherin EC domains contains around 110 amino acids, the contour length of each unfolded EC domain should be approximately 42 nm. In the native state, the physical size of each domain is about 3–5 nm [38,39]; thus, the change in contour length, ΔL, for the one-step unfolding of each EC domain would be expected to be the difference in these measurements; i.e., about ~ 38 nm. As shown in the insets of Figs. 3a and b, the contour length changes (ΔL) of most of the unfolding events were smaller than 38 nm. The small ΔL indicates that there are stable intermediate states along the unfolding pathways and, in most cases, partial unfolding of the EC domains was observed. This is consistent with the SMD simulation results of the first two EC domains of cadherins [40].

To further explore the mechanical stability of E-cadherin at a force condition close to that observed *in vivo* [41], Magnetic

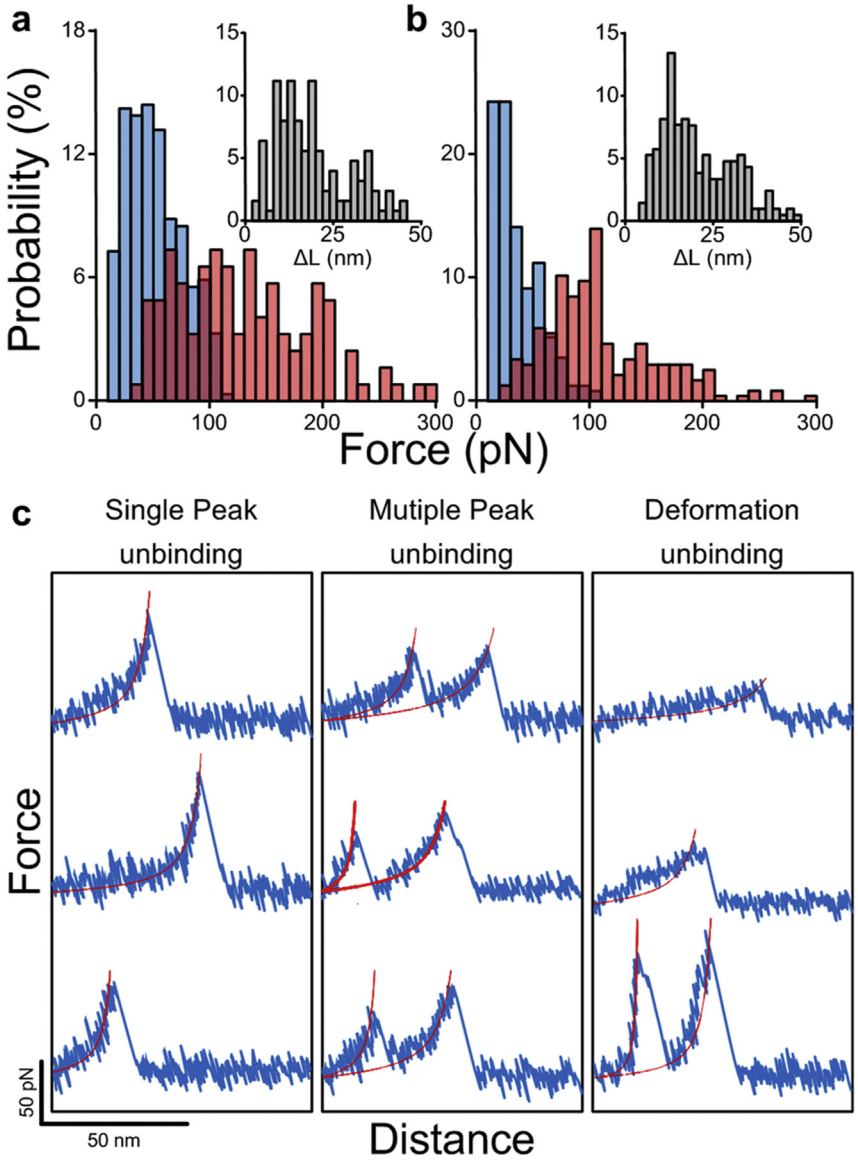

Fig. 3. Indication of unfolding occurs prior to unbinding. (a) Histograms of unbinding forces after a 2-seconds contact (blue) and the forces of the first unfolding events (red) for E-cadherins. The probability that unfolding occurs prior to unbinding calculated from the overlap area is 12%. The inset shows the histogram of the ΔL of the first unfolding events. The total number of events for the unbinding and unfolding histograms are 379 and 117, respectively. (b) Histograms of unbinding forces after a 2-seconds contact (blue) and unfolding (red) forces for cadherin 7. The probability that unfolding occurs prior to unbinding calculated from the overlap area is 6%. The inset shows the histogram of the ΔL of the first unfolding peak. The total number of events of unbinding and unfolding histograms are 366 and 226, respectively. (For interpretation of the references to colour in this figure legend, the reader is referred to the web version of this article.)

tweezers/evanescent nanometry was used to unfold the EC domains at a force of 5 ± 3 pN (SD). Specific biochemical linkage groups were used at both terminals of the full E-cadherin extracellular segment to fix individual molecules between the magnetic beads and the quartz substrate. In this way, only the functionalised proteins, i.e., E-cadherin EC domains in this case, were stretched by magnetic tweezers [42]. Both unfolding and refolding events were observed in the same trajectory of pulling EC domains by magnetic tweezers (Fig. 4b, insert). The contour length changes, ΔL, in unfolding and refolding displayed a broad distribution (Figs. 4a and b). Similarly, most unfolding events in magnetic tweezers measurements resulted in ΔL of less than 38 nm, confirming the partial unfolding of EC domains observed in the AFM experiments. The dwell time, t, between a pair of consequent events is relevant to the rates of events [31]. The histograms of the dwell time for folding/unfolding events (Figs. 4c and d) were fitted by single-exponential decay with unfolding and refolding rates of ~0.027 s^{-1} and ~0.032 s^{-1}, respectively.

3.3. Rupture of the homophilic interactions and unfolding of EC domains

Interestingly, for both cadherin types, the histograms of the unfolding and unbinding forces exhibited a partial overlap. From the histograms, the probability that the partial unfolding of the EC domains happens before the rupture of the homophilic interaction was estimated to be 12% and 6% for E-cadherin and cadherin 7, respectively (see Methods in File S1). Also, some trajectories show multiple force peaks. It is very difficult to distinguish whether these force peaks correspond to the breakage of multiple binding or partial unfolding of EC domains. Statistically, the ratios of pulling trajectories with multiple peaks were 15% for E-cadherin and 13% for cadherin 7, which are much higher than the multiple binding probabilities predicted by Poisson statistics, 5% and 6%, respectively. Thus, some of these multiple force peaks are probably the observation of partial unfolding of EC domains. In addition, some of the unbinding trajectories, the curve before rupture deviated from that predicted by the worm-like-chain (WLC) model, indicating the deformation of molecular structures. Some examples of multiple-peaked trajectory are shown in Fig. S2.

4. Discussion

4.1. The binding force of E-cadherin is stronger than cadherin 7

The AFM results show that the interaction between E-cadherin (type I) is stronger than that between cadherin 7 (type II), as the average unbinding force is higher for E-cadherins (Fig. 2). This is in agreement with *in vivo* cell adhesion measurements [6,7]. However, here AFM experiments are measuring the unbinding force at single-

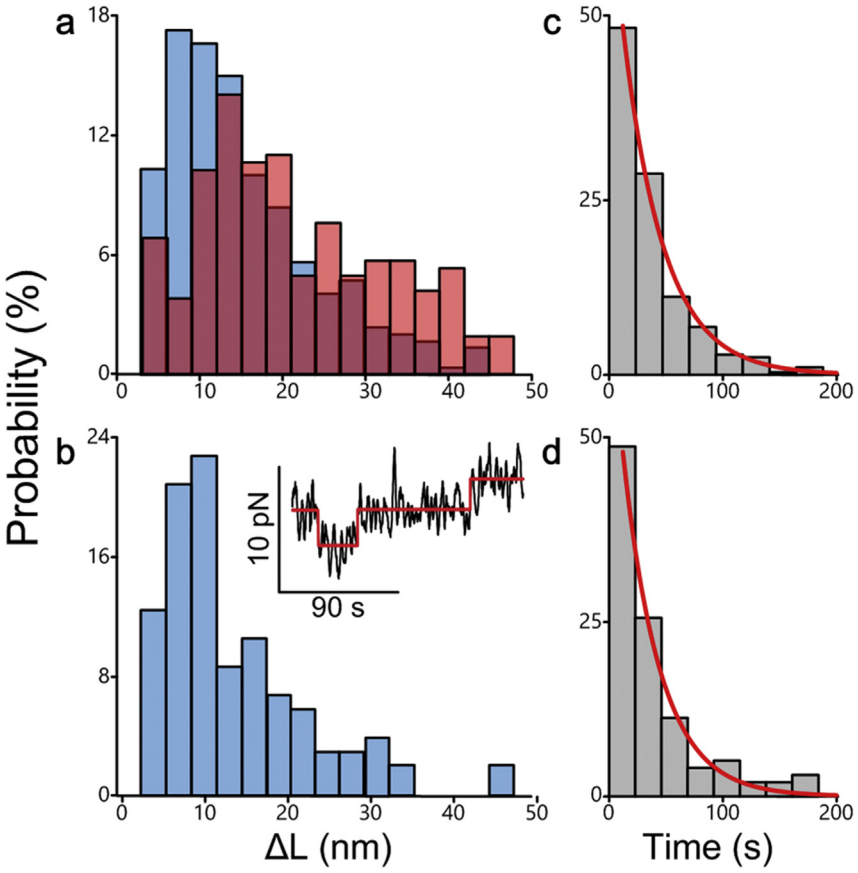

Fig. 4. Forced unfolding of extracellular domains of E-cadherins by magnetic tweezers. (a) Histogram of change in contour length, ΔL, for unfolding events in magnetic tweezers (blue). The ΔL was calculated from the extension change and force using the Worm-Like-Chain (WLC) model, with a persistance length of 0.38 nm. The total number of events is 303. The histogram of ΔL measured by AFM is shown in red, with 263 total number of events. Two histograms show a similar distribution. (b) The histogram of ΔL for refolding events. The total number of events is 108. The inset shows a typical extension-time trajectory with both unfolding and refolding events in a HEPES buffer with pH 7.2 and 1 mM Ca^{2+}. The external force was kept at 5 ± 3 pN (SD). The unfolding/refolding steps were found by a reported algorithm [60] (red step) (c) and (d) show the dwell time distributions of unfolding and refolding rates of 0.028 s^{-1} and 0.031 s^{-1}, respectively, by exponential fitting (red curves). (For interpretation of the references to colour in this figure legend, the reader is referred to the web version of this article.)

molecule level, so strengthening mechanisms at the cellular level, e.g. lateral clusters [43,44] and other cytoplasmic mechanosensing proteins [19–21], are absent. This indicates that the stronger unbinding force than that of cadherin 7 is an intrinsic property of E-cadherin dimer and should be determined by the structure and organisation of the E-cadherin EC domains. On the other hand, crystallographic data suggest that both type I and type II cadherins form dimers by a strand-swapping mechanism [13,14]. The larger buried surface in the strand-swapped dimer of type II cadherin suggests the better stability, consistent with *in vitro* ultracentrifugation experiments [17]. This seems contradictory to the lower unbinding forces observed in AFM experiments for cadherin 7 (type II), as well as the cell adhesion measurements [6,7].

4.2. Strengthening of cadherin adhesion over time and by forces

Further investigations on the homophilic interactions of E-cadherin and cadherin 7 show a strengthening effect for both E-cadherin and cadherin 7 homophilic interactions over contact-time. By changing the contact time from 2 s to 10 s before measuring the unbinding forces (Fig. 2) in AFM experiments, we observed a trend in the increment of the percentage of high unbinding force for both E-cadherin and cadherin 7. This is similar to the observation at the cellular level, where the dual-pipette assay experiments show that the unbinding force between cadherin-expressing cells keeps increasing in 30 min for E-cadherin and 100 min for cadherin 7 respectively after contact [45]. Our results suggest that such strengthening of cadherin homophilic binding over time is an inherent molecular property and may contribute to the strengthening effect of cadherin-mediated cell adhesion.

In addition, the AFM experiments with the pull-release-pull cycles reveal that pre-pulling at a force of 25 pN can strengthen the binding between E-cadherin EC domains and cause a higher probability of large unbinding forces (Fig. 2). This strengthening effect by force is more significant than that observed over time, indicating a substantial role of mechanical force on the homophilic interaction of E-cadherins. Though the same stretching and release cycles may not occur at native state in cells *in vivo* experiments at the cellular [46] and molecular [18] levels have shown that the cytoskeleton exerts tension forces on cadherins. Thus, this force-strengthening mechanism probably is critical for the rapid and strong adhesion of E-cadherins. In contrast, the force-strengthening effect is absent in case of cadherin 7. Therefore, at the molecular level, force can differentiate the homophilic binding of E-cadherin and cadherin 7, and in turn this should be one of the factors leading to the significant difference in cell adhesions mediated by these two types of cadherins [6]. In other words, the role of force to change conformation of cadherins during the dynamics of cell adhesion should not be neglected, as so far it is.

4.3. Force can deform/unfold cadherin EC domains

It is well established that stretching forces can deform or unfold proteins [47,48]. It has also been shown that force can activate vinculin binding to talin and α-catenin by unfolding them to expose the binding sites [49,50]. At cadherin-mediated cell adhesion, cadherins are also force-bearing nodes similar to talins/α-catenins, so it is very interesting to find that cadherin EC domains undergo conformational changes, i.e. partial unfolding and deformations, under external forces by both the AFM and magnetic tweezers experiments. The distribution of the ΔL in these unfolding events (Fig. 4a and Fig. S3 in Supporting Informations) is similar to the SMD simulation results [39,40,51], all below the contour length of individual EC domain, ~38 nm. This means that each EC domain usually won't unfold completely in one step, but go through one or a few stable intermediate states. The distribution of the unfolding forces in AFM experiments overlaps partially with that of the unbinding forces in Fig. 3. From the overlap, the chance of a partial unfolding event before an unbinding event in AFM experiments is estimated to be 12% and 6% for E-cadherin and cadherin 7, respectively. In addition, the deformation of the EC domains without unfolding was also occasionally observed prior to bond rupture in the unbinding force vs. extension trajectories for both cadherin types (Fig. S2), as implied by the deviation from the WLC model in the curve prior to the peak.

In magnetic tweezers experiment, the E-cadherin EC domains were able to unfold at a force of 5 ± 3pN (SD), which is close to the tension forces applied by the cytoskeleton on E-cadherin *in vivo* [41]. At such a low force, the unfolding and refolding rates were both around 0.03 sec^{-1}, which is not slower than the turnover rate of E-cadherin measured *in vivo* [52–54]. The maturation process of junctions takes even longer, ~30 min for E-cadherin [6]. All of these results indicate that there is an unnegligible probability for the conformational change of EC domains prior to the rupture of their homophilic interactions during the initial phase of cell adhesion dynamics.

4.4. Force is essential in strengthening of cell adhesion

Conformational change of the EC domains may result in stronger bonds between E-cadherins, e.g. the catch-bond model proposed by Rakshit et al. There may also be other molecular mechanism involved. For example, the conformational change can expose extra hydrophobic surfaces, some of which may become alternate binding sites, just like the case of amyloid aggregates, which are formed from inter-molecular β-type interactions of unfolded normal proteins. In contrast, type II cadherins unfold in different pathways [55], leading to different exposed intermediate surfaces, likely unsuitable for additional binding. Nevertheless, the force triggered strengthening effect at the molecular level may exist *in vivo* and closely correlates with cytoskeleton, as evidenced by the following facts: 1) *in vivo* experiments at the cellular [46] and molecular [18] levels have shown that the cytoskeleton exerts tension forces on cadherins; 2) the unbinding force of individual E-cadherin interactions measured between single cells [56] is higher than that measured in our experiments as well as those from other studies for isolated EC-domains [34,36,37] at the similar loading rate; 3) force can trigger a series of conformational changes that could, in turn, cause bond formation or junction remodelling [20]; 4) the junctions between E-cadherin-expressing cells and stiff gel were stronger than those established with a soft gel [21].

Nevertheless, cadherin-mediated cell adhesion is a complicated process. So far many related mechanisms have been proposed, e.g. catch bonds of X-dimers, the involvement of the last three domains [30], the conformational changes in the cytoplasmic region, cytoplasmic linker proteins, GTPase activity and the network/cluster of *trans*- and *cis*-interactions of cadherins [24,45,57,58], as well as external forces. We believe that all of these mechanisms/factors may work together in cadherin-mediated cell adhesions, and the absence of one or more of these mechanisms/factors may result in a significant change in the adhesive strength.

In summary, our molecular force experiments showed varied strength in the homophilic interactions between the EC domains of E-cadherin and cadherin 7, as well as different mechanical stability of their EC domains. Even in the absence of the cytoplasmic region, individual E-cadherin (type I) displays a stronger unbinding force than cadherin 7 (type II). External forces applied by the AFM cantilever were also found to strengthen the E-cadherin interactions rather than that between cadherin 7. In addition, the results from the unfolding experiments suggest that the stability of

cadherin EC domains are not enough to ensure their integrity prior to the rupture of their homophilic interaction, and thus the chance of partial unfolding/deformation of these EC domains is not negligible. Furthermore, magnetic tweezers experiments demonstrated that partial unfolding of EC domains can take place at a force close to that borne by the cytoskeleton *in vivo*. Based on these findings, we propose that force play an essential role on differentiating the homophilic binding of various cadherins, i.e. type I and type II cadherins, as well as cell adhesion they mediate. This is the first attempt from such a more physical perspective to uncover the detailed mechanisms of cadherin-mediated adhesion.

Acknowledgements

We gratefully acknowledge support from the Research Start Fund for Talent Recruitment, Chongqing University, China, and the seed grant (WBS R-714-002-007-271) from the Mechanobiology Institute, Singapore.

Appendix A. Supplementary data

Supplementary data related to this article can be found at doi: 10.1016/j.abb.2015.10.008.

References

[1] M. Takeichi, K. Abe, Synaptic contact dynamics controlled by cadherin and catenins, Trends Cell Biol. 15 (2005) 216–221.
[2] B.M. Gumbiner, Regulation of cadherin-mediated adhesion in morphogenesis, Nat. Rev. Mol. Cell Biol. 6 (2005) 622–634.
[3] R. Umbas, et al., Expression of the cellular adhesion molecule E-cadherin is reduced or absent in high-grade prostate cancer, Cancer Res. 52 (1992) 5104–5109.
[4] U. Cavallaro, B. Schaffhauser, G. Christofori, Cadherins and the tumour progression: is it all in a switch? Cancer Lett. 176 (2002) 123–128.
[5] T.J. Boggon, et al., C-cadherin ectodomain structure and implications for cell adhesion mechanisms, Science 296 (2002) 1308–1313.
[6] Y.S. Chu, et al., Prototypical type I E-cadherin and type II cadherin-7 mediate very distinct adhesiveness through their extracellular domains, J. Biol. Chem. 281 (2006) 2901–2910.
[7] S. Dufour, et al., Differential function of N-cadherin and cadherin-7 in the control of embryonic cell motility, J. Cell Biol. 146 (1999) 501–516.
[8] M. Takeichi, Cadherins: a molecular family important in selective cell-cell adhesion, Annu. Rev. Biochem. 59 (1990) 237–252.
[9] M. Overduin, et al., Solution structure of the epithelial cadherin domain responsible for selective cell adhesion, Science 267 (1995) 386–389.
[10] Y. Shimoyama, et al., Identification of three human type-II classic cadherins and frequent heterophilic interactions between different subclasses of type-II classic cadherins, Biochem. J. 349 (2000) 159–167.
[11] S. Posy, L. Shapiro, B. Honig, Sequence and structural determinants of strand swapping in cadherin domains: do all cadherins bind through the same adhesive interface? J. Mol. Biol. 378 (2008) 954–968.
[12] O.J. Harrison, et al., Two-step adhesive binding by classical cadherins, Nat. Struct. Mol. Biol. 17 (2010), 348–U121.
[13] S.D. Patel, et al., Cadherin-mediated cell-cell adhesion: sticking together as a family, Curr. Opin. Struct. Biol. 13 (2003) 690–698.
[14] S.D. Patel, et al., Type II cadherin ectodomain structures: implications for classical cadherin specificity, Cell 124 (2006) 1255–1268.
[15] S. Rakshit, et al., Ideal, catch, and slip bonds in cadherin adhesion, Proc. Natl. Acad. Sci. U. S. A. 109 (2012) 18815–18820.
[16] K. Manibog, et al., Resolving the molecular mechanism of cadherin catch bond formation, Nat. Commun. 5 (2014) 3941.
[17] P. Katsamba, et al., Linking molecular affinity and cellular specificity in cadherin-mediated adhesion, Proc. Natl. Acad. Sci. U. S. A. 106 (2009) 11594–11599.
[18] N. Borghi, et al., E-cadherin is under constitutive actomyosin-generated tension that is increased at cell-cell contacts upon externally applied stretch, Proc. Natl. Acad. Sci. U. S. A. 109 (2012) 12568–12573.
[19] Q. le Duc, et al., Vinculin potentiates E-cadherin mechanosensing and is recruited to actin-anchored sites within adherens junctions in a myosin II-dependent manner, J. Cell Biol. 189 (2010) 1107–1115.
[20] D.E. Leckband, et al., Mechanotransduction at cadherin-mediated adhesions, Curr. Opin. Cell Biol. 23 (2011) 523–530.
[21] H. Tabdili, et al., Cadherin-dependent mechanotransduction depends on ligand identity but not affinity, J. Cell Sci. 125 (2012) 4362–4371.
[22] Z. Liu, et al., Mechanical tugging force regulates the size of cell-cell junctions, Proc. Natl. Acad. Sci. 107 (2010) 9944–9949.
[23] B. Ladoux, et al., Strength dependence of cadherin-mediated adhesions, Biophysical J. 98 (2010) 534–542.
[24] Y.I. Petrova, M.M. spano, B.M. Gumbiner, Conformational epitopes at cadherin calcium-binding sites and p120-catenin phosphorylation regulate cell adhesion, Mol. Biol. Cell 23 (2012) 2092–2108.
[25] S. Graslund, et al., Protein production and purification, Nat. Methods 5 (2008) 135–146.
[26] B. Shrestha, C. Smee, O. Gileadi, Baculovirus expression vector system: an emerging host for high-throughput eukaryotic protein expression, Methods Mol. Biol. 439 (2008) 269–289.
[27] S. van den Berg, et al., Improved solubility of TEV protease by directed evolution, J. Biotechnol. 121 (2006) 291–298.
[28] Y. Jiang, et al., Specific aptamer-protein interaction studied by atomic force microscopy, Anal. Chem. 75 (2003) 2112–2116.
[29] R. Roy, S. Hohng, T. Ha, A practical guide to single-molecule FRET, Nat. Methods 5 (2008) 507–516.
[30] Q.M. Shi, et al., Allosteric cross talk between cadherin extracellular domains, Biophysical J. 99 (2010) 95–104.
[31] R. Liu, et al., Mechanical characterization of protein L in the low-force regime by electromagnetic tweezers/evanescent nanometry, Biophys. J. 96 (2009) 3810–3821.
[32] J. Huang, et al., Differential regulation of adherens junction dynamics during apical-basal polarization, J. Cell Sci. 124 (2011) 4001–4013.
[33] C. Verbelen, H.J. Gruber, Y.F. Dufrene, The NTA-HiS(6) bond is strong enough for AFM single-molecular recognition studies, J. Mol. Recognit. 20 (2007) 490–494.
[34] Y.X. Zhang, et al., Resolving cadherin interactions and binding cooperativity at the single-molecule level, Proc. Natl. Acad. Sci. U. S. A. 106 (2009) 109–114.
[35] J. Wong, A. Chilkoti, V.T. Moy, Direct force measurements of the streptavidin-biotin interaction, Biomol. Eng. 16 (1999) 45–55.
[36] M.V. Bayas, et al., Lifetime measurements reveal kinetic differences between homophilic cadherin bonds, Biophys. J. 90 (2006) 1385–1395.
[37] E. Perret, et al., Trans-bonded pairs of E-cadherin exhibit a remarkable hierarchy of mechanical strengths, Proc. Natl. Acad. Sci. U. S. A. 101 (2004) 16472–16477.
[38] J. Oroz, et al., Nanomechanics of the cadherin ectodomain "CANALIZATION" BYCa2 BINDING results IN A new mechanical element, J. Biol. Chem. 286 (2011) 9405–9418.
[39] M. Sotomayor, K. Schulten, The allosteric role of the Ca2+ switch in adhesion and elasticity of C-cadherin, Biophysical J. 94 (2008) 4621–4633.
[40] R.C. Liu, F. Wu, J.P. Thiery, Remarkable disparity in mechanical response among the extracellular domains of type I and II cadherins, J. Biomol. Struct. Dyn. 31 (2013) 1137–1149.
[41] N. Borghi, et al., E-cadherin is under constitutive actomyosin-generated tension that is increased at cell-cell contacts upon externally applied stretch, Proc. Natl. Acad. Sci. U. S. A. 109 (2012) 12568–12573.
[42] H. Chen, et al., Improved high-force magnetic tweezers for stretching and refolding of proteins and short DNA, Biophysical J. 100 (2011) 517–523.
[43] Y. Wu, et al., Transforming binding affinities from three dimensions to two with application to cadherin clustering, Nature 475 (2011) 510–513.
[44] O.J. Harrison, et al., The extracellular architecture of adherens junctions revealed by crystal structures of type I cadherins, Structure 19 (2011) 244–256.
[45] Y.S. Chu, et al., Force measurements in E-cadherin-mediated cell doublets reveal rapid adhesion strengthened by actin cytoskeleton remodeling through Rac and Cdc42, J. Cell Biol. 167 (2004) 1183–1194.
[46] V. Maruthamuthu, et al., Cell-ECM traction force modulates endogenous tension at cell-cell contacts, Proc. Natl. Acad. Sci. U. S. A. 108 (2011) 4708–4713.
[47] T.E. Fisher, et al., The study of protein mechanics with the atomic force microscope, Trends Biochem. Sci. 24 (1999) 379–384.
[48] M. Rief, et al., Reversible unfolding of individual titin immunoglobulin domains by AFM, Science 276 (1997) 1109–1112.
[49] A. del Rio, et al., Stretching single talin rod molecules activates vinculin binding, Science 323 (2009) 638–641.
[50] M. Yao, et al., Force-dependent conformational switch of alpha-catenin controls vinculin binding, Nat. Commun. 5 (2014) 4525.
[51] M. Sotomayor, D.P. Corey, K. Schulten, In search of the hair-cell gating spring elastic properties of ankyrin and cadherin repeats, Structure 13 (2005) 669–682.
[52] M. Canel, et al., Use of photoactivation and photobleaching to monitor the dynamic regulation of E-cadherin at the plasma membrane, Cell Adh Migr. 4 (2010) 491–501.
[53] S. Yamada, et al., Deconstructing the cadherin-catenin-actin complex, Cell 123 (2005) 889–901.
[54] S. de Beco, et al., Endocytosis is required for E-cadherin redistribution at mature adherens junctions, Proc. Natl. Acad. Sci. U. S. A. 106 (2009) 7010–7015.
[55] L. Horvath, et al., Engineering an in vitro air-blood barrier by 3D bioprinting, Sci. Rep. 5 (2015) 7974.
[56] P. Panorchan, et al., Single-molecule analysis of cadherin-mediated cell-cell adhesion, J. Cell Sci. 119 (2006) 66–74.
[57] O.J. Harrison, et al., The extracellular Architecture of Adherens junctions revealed by Crystal structures of type I cadherins, Structure 19 (2011) 244–256.

[58] G.S. Brigidi, S.X. Bamji, Cadherin-catenin adhesion complexes at the synapse, Curr. Opin. Neurobiol. 21 (2011) 208–214.
[59] T.E. Fisher, et al., The study of protein mechanics with the atomic force microscope, Trends Biochem. Sci. 24 (1999) 379–384.
[60] J.W. Kerssemakers, et al., Assembly dynamics of microtubules at molecular resolution, Nature 442 (2006) 709–712.